Published in final edited form as:
J Mol Biol. 2009 July 17; 390(3): 380–393. doi:10.1016/j.jmb.2009.05.007.

Kinetic Buffering of Cross Talk between Bacterial Two-Component Sensors

Eli S. Groban[1], **Elizabeth J. Clarke**[1], **Howard M. Salis**[2], **Susan M. Miller**[1,2], and **Christopher A. Voigt**[1,2,*]

J. Karn

[1]Graduate Group in Biophysics, University of California, San Francisco, San Francisco, CA 94158, USA

[2]Department of Pharmaceutical Chemistry, University of California, San Francisco, San Francisco, CA 94158, USA

Abstract

Two-component systems are a class of sensors that enable bacteria to respond to environmental and cell-state signals. The canonical system consists of a membrane-bound sensor histidine kinase that autophosphorylates in response to a signal and transfers the phosphate to an intracellular response regulator. Bacteria typically have dozens of two-component systems. The key questions are whether these systems are linear and, if they are, how cross talk between systems is buffered. In this work, we studied the EnvZ/OmpR and CpxA/CpxR systems from *Escherichia coli*, which have been shown previously to exhibit slow cross talk *in vitro*. Using *in vitro* radiolabeling and a rapid quenched-flow apparatus, we experimentally measured 10 biochemical parameters capturing the cognate and non-cognate phosphotransfer reactions between the systems. These data were used to parameterize a mathematical model that was used to predict how cross talk is affected as different genes are knocked out. It was predicted that significant cross talk between EnvZ and CpxR only occurs for the triple mutant Δ*ompR* Δ*cpxA* Δ*actA-pta*. All seven combinations of these knockouts were made to test this prediction and only the triple mutant demonstrated significant cross talk, where the *cpxP* promoter was induced 280-fold upon the activation of EnvZ. Furthermore, the behavior of the other knockouts agrees with the model predictions. These results support a kinetic model of buffering where both the cognate bifunctional phosphatase activity and the competition between regulator proteins for phosphate prevent cross talk *in vivo*.

Keywords

two-component systems; systems biology; synthetic biology; computational biology; genetic circuits

Introduction

Bacteria use a variety of sensing mechanisms to respond to changes in the environment and the cell state. A ubiquitous motif is the two-component system, where one protein acts as the sensor and the other as a signal carrier.[1–3] Upon receiving a signal, the sensor autophosphorylates at a histidine residue and transfers the phosphate to the signal carrier, a

*Corresponding author. cavoigt@picasso.ucsf.edu..

Supplementary Data

Supplementary data associated with this article can be found, in the online version, at doi:10.1016/j.jmb.2009.05.007

response regulator protein.[4,5] The response regulator can either affect a larger signaling network, as in chemotaxis, or alter gene expression by binding to DNA.[1,6–9] Two-component systems are capable of responding to a wide variety of signals, including temperature, touch, light, metals, dissolved gasses, chemicals, membrane stress, antibiotics, nutrients, pH, and nitrogen sources and are involved in many cellular processes, including cell division, motility, pathogenesis, biofilm formation, and cell–cell communication.[9–26]

Two-component systems are remarkably modular—a property that is being increasingly exploited in engineering applications.[27–30] The N-terminal domain of the sensor kinase, which responds to the extracellular signal, shows the most diversity.[1,2] In contrast, the C-terminal histidine kinase domains and the N-terminal response regulator domains share highly conserved amino acid sequences, and many structural studies show only subtle differences in three-dimensional shape among response regulators in *Escherichia coli*.[31–34] This conservation enables domain swapping to be used to rewire pathways to mix and match inputs and outputs.[35–40]

Because of the number of simultaneously expressed systems and the strong conservation in the sequence and structure, it seems plausible that cross-reactions would occur frequently between systems.[41–45] These could manifest as a single kinase phosphorylating multiple response regulators, or, conversely, a single regulator could be phosphorylated by multiple kinases. In contrast, two-component systems could behave linearly, where a histidine kinase only phosphorylates its cognate response regulator. Given the similarity between systems, there would have to be some sort of buffering mechanism for linearity to be preserved.[41,46,47]

Cross talk between non-cognate pairs has been observed *in vitro*. Yamamoto *et al*. assayed 25 histidine kinases from *E. coli* against the 34 *E. coli* response regulators.[49] After a 30-s incubation time, 11 of the 34 response regulators can be phosphorylated by more than one histidine kinase. However, there are only a few promiscuous kinases, so of 692 possible cross-talk pairs, only 3% showed *in vitro* cross talk. Skerker *et al*. assayed the EnvZ, CpxA, and CheA kinases against a panel of all response regulators from *E. coli*.[50] After 10 s, EnvZ fully phosphorylated OmpR, but it required 1 h for non-cognate phosphorylation of CpxR to occur. This suggests that the non-cognate transfer is too slow to be relevant *in vivo*.

Several theories have been proposed to explain how two-component systems could buffer *in vivo* the slow cross talk observed *in vitro*. Alves and Savageau proposed that buffering could emerge from the ability of the histidine kinase to both phosphorylate and dephosphorylate the response regulator (a bifunctional interaction).[46] Using a mathematical model, they demonstrated that the phosphatase function could decrease the background phosphorylation of the response regulator, thus reducing cross talk. This is supported in recent work where it was demonstrated that cross talk between CpxA and OmpR *in vivo* requires that the EnvZ sensor and CpxR regulator be knocked out.[47]

Skerker *et al*. argued that each kinase has a “kinetic preference” for its cognate substrate.[50] They postulated that subtle amino acid differences in the binding interface between the kinase and the response regulator affect the K_m. If the correct response regulator interacts for a longer time with its kinase, this both prevents access to the kinase by the incorrect substrate and drains the kinase of all available phosphate, resulting in phosphorylation of only the correct response regulator. To support this hypothesis, they made small amino acid changes to the kinase at the binding interface, which resulted in a shift in kinetic preference that altered specificity.[42]

In this study, we characterized the interactions between the *E. coli* EnvZ/OmpR and CpxA/CpxR two-component systems.[4,8,51] These systems respond to many extracellular signals and are often labeled as osmosensors.[8,52] They also co-regulate many cellular responses, including flagella assembly, pathogenesis, outer membrane porins, and biofilm formation.[8,11,15,53]

OmpR and CpxR often bind to different operators within the same promoter.[54] The phosphotransfer domains share the most similarity among *E. coli* two-component systems, sharing 31% amino acid identity for the kinase domain of the sensor histidine kinase and 50% identity between the receiver domains of the response regulators.[55] It has been shown previously that EnvZ can phosphorylate CpxR *in vitro*, albeit at a much slower rate than OmpR.[49,50]

Both EnvZ and CpxA are bifunctional histidine kinases, containing both kinase and phosphatase activities.[56–58] Interestingly, the OmpR and CpxR response regulator proteins respond differently in the absence of their cognate sensor. In the absence of EnvZ, or when EnvZ is not stimulated, OmpR-P levels are very low.[8,35] EnvZ then acts as a kinase when stimulated. In contrast, CpxR exists in an active phosphorylated state in the absence of CpxA and maintains a basal level of activity in the presence of the CpxA kinase.[59,60]

We performed a comprehensive study of the interactions between the EnvZ/OmpR and CpxA/CpxR two-component systems using a combination of *in vitro* and *in vivo* experiments (Fig. 1). We directly measured *in vitro* three classes of kinetic rates: the phosphorylation and dephosphorylation rates of the response regulator by both cognate and non-cognate histidine kinases and the acetyl-phosphate-dependent autophosphorylation rate of the response regulator. These constants allowed us to parameterize a predictive model for the response regulator phosphorylation state. We used the model to predict the behavior of a series of knockouts that each removes one or more buffering mechanisms. These predictions were confirmed with *in vivo* promoter measurements that show significant cross talk only when all buffering mechanisms are removed.

Results

In vitro phosphotransfer experiments

We measured 10 kinetic constants (k_1–k_{10}; Fig. 2) *in vitro* using purified proteins, radiolabeled phosphate, and a rapid quenched-flow apparatus for reactions that occur on fast timescales (Materials and Methods). For the kinases, only the cytoplasmic portion was purified as data from previous studies show that this portion is active *in vitro*.[8,49,50,61] Cognate (k_1 and k_6) and non-cognate (k_2 and k_7) kinase rates were measured by radiolabeling the histidine kinase and observing phosphotransfer when the response regulator was introduced. Purified histidine kinase was labeled by exposing it to [γ-^{32}P]ATP for 30 min, allowing it to autophosphorylate. The phosphorylated kinase was washed to remove all free ATP before adding a 10-fold excess of response regulator protein and allowing the reaction to proceed to completion in order to observe single turnover. A rapid quenched-flow apparatus was used for reactions that were complete in less than 1 s.

The response regulators were labeled and then mixed with histidine kinase to measure the cognate (k_3 and k_8) and non-cognate (k_4 and k_9) phosphatase rates. Previous studies demonstrated that response regulators can be phosphorylated by using acetyl phosphate *in vitro*.[62,63] As ^{32}P-labeled acetyl phosphate is not commercially available, this small molecule was synthesized from radiolabeled (^{32}P-labeled) phosphate and acetic anhydride.[63] Response regulator proteins were exposed to ^{32}P-labeled acetyl phosphate for 1 h and then mixed with histidine kinase. The loss of phosphate from the response regulator was used to calculate the phosphatase rate. These experiments provide data to determine rates of kinase-dependent response regulator dephosphorylation. In addition, the ^{32}P-labeled acetyl phosphate is used to determine the autophosphorylation rates of the response regulators (k_5 and k_{10}).

The rate constants k_1–k_{10} are determined by fitting the experimental phosphotransfer curves to the solution of a system of ordinary differential equations (ODEs). For each *in vitro*

phosphotransfer assay, a linear ODE that describes the dynamics of the phosphorylation and dephosphorylation of the response regulator is derived. An analytical algebraic solution to this equation relates the fraction of phosphorylated response regulator to time and the kinetic constants of each reaction in the assay. This procedure was repeated for all 10 phosphotransfer assays, resulting in a system of algebraic equations that describe the dynamics of phosphorylated OmpR and CpxR under each reaction condition. The values of the rate constants that best reproduced the phosphotransfer curves were determined by minimizing the least-squares residual between the algebraic solution and the experimental data (Materials and Methods). Overall, the data fitting required 10 differential equations with 10 parameters, k_1–k_{10}, and yielded a unique set of parameter values that reproduces all of the phosphotransfer dynamics. The constants k_5 and k_{10} appear in multiple equations. The solutions to this fitting procedure are shown as the curves in Fig. 2 and in Table 1.

EnvZ and CpxA phosphorylate their cognate response regulator proteins very rapidly. The EnvZ/OmpR reaction reaches completion in less than 40 ms, with a forward rate constant of $k_1 = 102\ s^{-1}\ M^{-1}$ (Fig. 2a). CpxA phosphorylates CpxR rapidly as well, although with a lower rate constant of $k_6 = 28.5\ s^{-1}\ M^{-1}$ (Fig. 2b). These numbers are faster than estimated in previous studies that could not achieve sub-second resolution.[4,49,50]

Non-cognate phosphorylation is much slower. The rate constants for OmpR phosphorylation by CpxA and CpxR phosphorylation by EnvZ are $k_2 = 0.003\ s^{-1}\ M^{-1}$ and $k_7 = 0.003\ s^{-1}\ M^{-1}$ (Fig. 2), which agree qualitatively with previous studies.[49,50] These represent a 33,000-fold difference in the rate of cognate *versus* non-cognate phosphorylation for OmpR and a 9300-fold difference for CpxR.

The cognate and non-cognate phosphatase reactions were also measured. EnvZ dephosphorylates OmpR with a rate constant of $k_3 = 0.003\ s^{-1}\ M^{-1}$ (Fig. 2a), which agrees with previous studies.[64] CpxA dephosphorylates CpxR on the same time-scale, with a rate of $k_8 = 0.003\ s^{-1}\ M^{-1}$ (Fig. 2b).[49] However, neither kinase can efficiently dephosphorylate its non-cognate response regulator ($k_4 = 0.0001\ s^{-1}\ M^{-1}$ and $k_9 = 0.0002\ s^{-1}\ M^{-1}$) (Fig. 2). It is noteworthy that the cognate dephosphorylation rates (k_3 and k_8) are nearly identical with the non-cognate phosphorylation rates (k_2 and k_7). This means that the bifunctional kinase activity is just strong enough to remove the phosphate that accumulates from cross-reactions, as predicted by Alves and Savageau.[46]

The rates of autophosphorylation by acetyl phosphate for OmpR and CpxR are the slowest contributions to response regulator phosphorylation, with rate constants of $k_5 = 0.001\ s^{-1}$ and $k_{10} = 0.001\ s^{-1}$, respectively (Fig. 2). These agree with published values for OmpR.[62] In the absence of any kinase, both OmpR-P and CpxR-P have an inherent autophosphatase rate that is negligible on the timescales observed. This is slower than that previously reported for OmpR-P.[56,62]

A mathematical model of the EnvZ/OmpR and CpxA/CpxR systems

A mathematical model was developed to determine the global network dynamics that emerge from the set of rate constants obtained *in vitro*. The model focuses on how the steady-state level of CpxR-P is affected by phosphate flux from EnvZ and is used to quantify how cross talk is affected by knocking out different components of the system. The model consists of a set of four differential equations,

$$\frac{dC_{OmpR-P}}{dt} = C_{OmpR}\left[k_1 C_{EnvZ-P} + k_2 C_{CpxA-P} + k_5\right] - C_{OmpR-P}\left[k_3 C_{EnvZ} + k_4 C_{CpxA}\right] - \gamma C_{OmpR-P}$$
$$\frac{dC_{CpxR-P}}{dt} = C_{CpxR}\left[k_6 C_{CpxA-P} + k_7 C_{EnvZ-P} + k_{10}\right] - C_{CpxR-P}\left[k_8 C_{CpxA} + k_9 C_{EnvZ}\right] - \gamma C_{CpxR-P}$$
$$\frac{dC_{EnvZ-P}}{dt} = I_{EnvZ} C_{EnvZ} - C_{EnvZ-P}\left[k_1 C_{OmpR} + k_7 C_{CpxR}\right] - \gamma C_{CpxR-P}$$
$$\frac{dC_{CpxA-P}}{dt} = I_{CpxA} C_{CpxA} - C_{CpxA-P}\left[k_6 C_{CpxA} + k_2 C_{OmpR}\right] - \gamma C_{CpxA-P}$$

and four mole conservation relations,

$$C_{OmpR,TOT} = C_{OmpR-P} + C_{OmpR}$$
$$C_{CpxR,TOT} = C_{CpxR-P} + C_{CpxR}$$
$$C_{EnvZ,TOT} = C_{EnvZ-P} + C_{EnvZ}$$
$$C_{CpxA,TOT} = C_{CpxA-P} + C_{CpxA}$$

where C represents the concentration of each species. According to Cai and Inouye, there are approximately 3000–4000 molecules of OmpR and 100 molecules of EnvZ in an *E. coli* cell.[65] We set $C_{OmpR,TOT}$ and $C_{CpxR,TOT}$ to 5 μM, which is 5000 molecules per cell. $C_{CpxA,TOT}$ is set to 0.5 μM, or 500 molecules per cell. Setting $C_{EnvZ,TOT}$ to 0.5 μM did not result in a model that qualitatively fit to our wild-type (WT) *in vivo* data. However, because TAZ is expressed from a multicopy plasmid with a strong promoter, we therefore increased $C_{EnvZ,TOT}$ to 2 μM, which improved the ability of the model to reproduce the initial fluorescence measurements in the WT strain. The kinase and phosphatase rates are described using second-order kinetics. The acetyl-phosphate transfer rate is described using pseudo-first-order kinetics, where the acetylphosphate concentration is lumped together with the transfer rate's kinetic constant.

The effects of cell growth are also included, using a doubling time of 30 min ($\gamma = 3.85 \times 10^{-4}$ s^{-1}). The parameters I_{EnvZ} and I_{CpxA} are set to 0.003 and 0.009 s^{-1}, respectively, and quantify the histidine autophosphorylation rates of the respective kinases, which were estimated based on previous measurements of the KinA histidine kinase from *Bacillus subtilis* and with the criterion that both kinases should never be fully phosphorylated *in vivo*.[48]

The differential equations are numerically integrated to generate dynamic profiles of the fraction of CpxR-P ($C_{CpxR\text{-}P}/C_{CpxR,TOT}$) that occurs *in vivo* under different knockout scenarios (Fig. 3a). The steady-state model solutions in the absence of active EnvZ are determined and EnvZ is then activated at the 6-min time point. After activation, the new steady-state model solutions are then determined the end points are shown in Fig. 3b.

For the WT, CpxR-P is insensitive to phosphate flux from EnvZ (Fig. 3a and b). In the modeling work, the WT contains the kinase domains of EnvZ, CpxA, OmpR, and CpxR response regulators. To knock out a protein in the model, we set the participating rate constants to zero. When the CpxA protein is removed ($k_2 = k_4 = k_6 = k_8 = 0$), the system responds in an unexpected way. We were expecting that this would enable cross talk from EnvZ. However, it produced an interesting phenotype where phosphate flux from EnvZ decreases the accumulation of CpxR-P (Δ*cpxA*; Fig. 3a and b). This occurs because, when present, OmpR acts as the sink for all of the phosphate from EnvZ. This leaves only the very weak phosphatase activity toward CpxR-P, which is very slow *in vitro*. This effect was confirmed *in vivo* (next section).

When OmpR is also removed from the model ($k_1 = k_2 = k_3 = k_4 = k_5 = 0$), this eliminates the inverse effect, and a small amount of cross talk is observed both in the presence and in the

absence of CpxA (Δ*ompR* Δ*cpxA* and Δ*ompR*; Fig. 3a and b). This cross talk occurs on a much slower timescale than what is observed for cognate transfer between EnvZ and OmpR (Figs. 2a and 3a). While we saw cross talk for these perturbations to the model, it was not observed *in vivo* (next section). Moreover, in all cases, knocking out OmpR in the model produces a small amount of cross talk from EnvZ to CpxR. This small effect was not observed *in vivo* (next section).

Finally, we predicted the effect of disrupting the autophosphorylation of OmpR and CpxR. We hypothesized that cross talk could be masked by the high background of CpxR-P that occurs when CpxA is removed. It has been shown previously that the autophosphorylation of response regulators can be disrupted by knocking out acetate kinase A and phosphotransacetylase (Δ*ackA-pta*).[60,66] This is incorporated into the model by setting $k_5 = k_{10} = 0$.

The disruption of autophosphorylation has no effect on the otherwise intact system (Δ*actA-pta*; Fig. 3a and b). It also has little effect on the mutant where OmpR is removed (Δ*ompR* Δ*actA-pta*). In both cases, the CpxR-P level is controlled by the kinase and phosphatase activities of the CpxA kinase, which is unaffected by the removal of acetyl-phosphate production. The Δ*actA-pta* Δ*cpxA* simulation shows a slight amount of cross talk in the presence of active EnvZ, yet, in its absence, CpxR is not phosphorylated. In the *ackA-pta/ cpxA* knockout scenario, the EnvZ kinase is the only possible source of phosphotransfer to CpxR. Thus, the model shows that when EnvZ is absent, CpxR remains unphosphorylated. When an active EnvZ is present in the model, CpxR becomes phosphorylated, yielding a small amount of cross talk. This level of cross talk was observed *in vivo* (next section).

We evaluated different single, double, and triple knockouts of *cpxA*, *ompR*, and *ackA-pta*. The model predicts that the system is incredibly robust to cross talk and that only a triple knockout should allow us to observe cross talk *in vivo* (Δ*ackA-pta* Δ*cpxA* Δ*ompR*; Fig. 3a and b). The background concentration of CpxR-P is reduced to zero by knocking out these pathways. With acetyl-phosphate synthesis and CpxA knocked out, EnvZ is the only source of phosphate for CpxR. Moreover, both OmpR, which is a competitor for phosphate, and CpxA, which serves as a CpxR-P phosphatase, are removed from the system. We sought to confirm this result *in vivo*.

Demonstration of cross talk *in vivo*

We monitored the *in vivo* phosphorylation states of OmpR and CpxR by following the activities of the *ompC* and *cpxP* promoters, respectively (Fig. 4a and b). These promoters were chosen because footprint experiments have demonstrated that the response regulator binds to specific sequences upstream of the – 35 site and they have been previously validated as readouts for OmpR-P and CpxR-P.[67,68] These promoters respond to conditions known to activate the systems as shown by both β-galactosidase and green fluorescent protein (GFP) reporter systems.[69–71]

We selectively activated the EnvZ/OmpR pathway in order to determine whether *in vivo* cross talk occurs between it and CpxA/CpxR. As there is no known ligand for the EnvZ kinase, we used a second-generation version of the hybrid kinase designed by Jin and Inouye that combines the transmembrane aspartate receptor with the kinase domain of the EnvZ kinase (TAZ) (Fig. 4c and d).[57] This hybrid kinase serves to selectively activate the EnvZ kinase domain and phosphorylate its cognate response regulator OmpR in the presence of the small molecule aspartate. We activated the EnvZ kinase using the TAZ construct and monitored the output levels of both the EnvZ/OmpR and CpxA/CpxR systems using the promoters *ompC* and *cpxP* to drive GFP expression, which is measured at the single-cell level using flow cytometry (Fig. 4d and g).

TAZ phosphorylates the OmpR response regulator in the presence of 5 mM aspartate *in vivo* in the WT (Fig. 4e and f). In the *in vivo* work, our reference to the WT really refers to a cell in which the EnvZ kinase has been knocked out and replaced with the TAZ kinase. Induction of TAZ via addition of 5 mM aspartate leads to a 34.7 ± 1.9-fold increase in induction of fluorescence by the *ompC* promoter, showing that the presence of aspartate and TAZ provides an active EnvZ kinase, defined as TAZ in the presence of aspartate. This activation is TAZ dependent, as a control strain lacking TAZ shows no activity at the *ompC* promoter (Fig. 4f). Δ*ompR* does not respond to TAZ, showing that the *ompC* promoter is specific to OmpR-P. Our use of GFP as a reporter for system activity, combined with flow cytometry, allowed us to conduct single-cell measurements. From these we found that cells containing the *ompC* promoter GFP fusions produce a single distribution in all cases (Fig. 4e).

In the WT, active EnvZ kinase does not affect the levels of CpxR-P response regulator *in vivo* (Fig. 4g–i). By monitoring the abundance of phosphorylated CpxR via the *cpxP* promoter and activating the EnvZ kinase, we were able to measure the presence or absence of cross talk between EnvZ and CpxR. We were unable to see a significant difference in *cpxP* activity in the presence of active EnvZ kinase.

We then constructed seven knockout mutants containing all possible combinations of Δ*cpxA*, Δ*ompR*, and Δ*ackA-pta* (Materials and Methods). In addition, EnvZ was also knocked out and TAZ was introduced on a plasmid. For each of the knockouts, the activity of the promoters is compared for the Δ*envZ* strain (–) and the addition of the TAZ and 5 mM aspartate (+) (Fig. 5).

The knockout Δ*cpxA* causes the level of CpxR-P to increase, as reflected by the increase in the *cpxP* promoter activity (Fig. 5). In the absence of the CpxA kinase, CpxR autophosphorylates using acetyl phosphate as a substrate and reaches a higher steady state. Notably, the experiments recover the decrease in activity from the addition of active EnvZ kinase as observed in the model (Fig. 3). The double knockout Δ*cpxA* Δ*ompR* strongly activates the *cpxP* promoter and is insensitive to active EnvZ kinase.

The Δ*ompR*, Δ*ackA-pta*, and Δ*ompR* Δ*ackA-pta* strains behave similarly with WT. The mathematical model correctly predicted the behavior of Δ*ackA-pta*. However, the model overestimated the effect of knocking out OmpR on these strains, where a small amount of cross talk is predicted but not observed.

The Δ*ackA-pta* Δ*cpxA* strain strongly decreases the amount of CpxR-P and the activity of the *cpxP* reporter. However, there is a small amount of cross talk observed, where active EnvZ kinase is able to phosphorylate CpxR and induce the *cpxP* promoter by 3.6 ± 0.2-fold. This is consistent with the prediction of the model (Fig. 3).

A Δ*ackA-pta* Δ*cpxA* Δ*ompR* triple knockout showed very strong EnvZ-dependent phosphorylation of CpxR *in vivo* (Fig. 5, panel 9). Inducing TAZ in this system caused a 370.4 ± 79.8-fold increase in *cpxP* activity. Moreover, according to the model, changes in TAZ expression may alter the magnitude of this increase but not the qualitative response. This system lacks two crucial mechanisms to prevent cross talk. First, it lacks the bifunctional phosphatase activity of CpxA. Second, it does not have the OmpR protein, allowing CpxR access to the active EnvZ kinase. In the WT system, CpxA serves as a phosphatase for CpxR and OmpR quickly removes phosphate from active EnvZ kinase. It is only by removing all possible mechanisms for insulation that we see a potent activation of CpxR by EnvZ *in vivo*. These buffering mechanisms are very effective, and a similar conclusion was found for the phosphorylation of OmpR by CpxA, where EnvZ and CpxR had to be knocked out to see cross talk.[47] Here, we have to make the additional deletion that affects the autophosphorylation of

CpxR in order to see cross talk from EnvZ because CpxR-P levels are high in the absence of CpxA.

Discussion

The field of systems biology often seeks to model global dynamical behaviors using sets of parameters obtained individually *in vitro*. An open question is whether the conditions *in vitro* sufficiently reflect the cellular environment for the parameters to be relevant. Here, we have completely characterized the phosphotransfer pathway of two interacting two-component systems. A set of rate constants obtained using purified protein *in vitro* was used to parameterize a mathematical model that correctly predicts the higher-order dynamical behavior of the system *in vivo*. The effect that the knockouts have on the signaling network could not be predicted from the individual parameters alone.

Here, we started with two systems that share a high degree of sequence similarity and for which cross talk had been previously demonstrated *in vitro*.[49,50] Remarkably, it required three knockouts to induce cross talk, which demonstrates the degree to which two-component systems are buffered. This is consistent with other recent observations, all of which point to phosphotransfer being linear in the native host.[47] There are other mechanisms by which cross talk can occur, including the inclusion of additional kinase domains in the sensor kinase that interact with other response regulators.[1,2,41] There are also examples of cytoplasmic adaptor proteins that integrate multiple sensors and then interact with a downstream response regulator. An example of this is the Spo0F protein in *B. subtilis*, which integrates multiple sensors and activates the Spo0A response regulator through the histidine phosphotransferase Spo0B.[72,73] However, unless there are additional domains or proteins involved in phosphotransfer, it would appear that the phosphotransfer that occurs in canonical two-component systems is remarkably linear.

The absence of *in vivo* cross talk arises from the combination of multiple factors: the large ratio of cognate to non-cognate kinase activity, the presence of a cognate phosphatase activity, and substrate competition. Through *in vitro* experiments, we have been able measure the biochemical kinetics underlying these interactions, and their combined effect is predicted by a mathematical model. It should be noted that it is likely that there will be differences between the parameters *in vivo* and *in vitro*—for example, the difference between the activity of a truncated histidine kinase domain and that of the full-length protein when stimulated. In this case, the model is robust to these potential differences.

Integrating two-component systems may play a critical role for bacteria to identify an environment. To this end, there are many promoters that contain multiple operators that bind different response regulators.[74–76] There are also genetic circuits that act as logic to integrate multiple inputs. An emerging conclusion is that much of the signal integration between two-component systems occurs on the transcriptional level.

The remarkable degree of buffering occurs due to a combination of kinetic interactions. We found that the bifunctional phosphatase activities of the sensors are just fast enough to remove the phosphates that get transferred via non-cognate interactions. This supports the theory put forward by Alves and Savageau.[46] However, when only this interaction is removed, significant cross talk does not occur. The removal of OmpR is critical for significant cross talk to occur. There is evidence that the response regulators act as phosphate sinks by preferentially interacting with their cognate sensor. Previous studies suggest that only 0.02% of EnvZ is phosphorylated *in vitro* and that OmpR preferentially interacts with phosphorylated EnvZ, leaving only the unphosphorylated EnvZ to act as a phosphatase to interact with non-cognate response regulators.[49,64,77] Our model does not include sequestration and the *in vitro*

experiments are with excess substrate, making it impossible to determine a K_m. Still, we saw evidence of this effect in the TAZ induction when CpxA was knocked out.

Programmable sensors are a key component for engineering bacteria.[78] The modularity of two-component systems makes them an intriguing target for engineering, where input signals can be rapidly connected to control different pathways through domain swapping.[35–40] In addition, two-component systems can generally be moved between species. This enables access to a diversity of sensing functions present in bacteria. However, it has been observed that after transfer, two-component systems can exhibit cross-reactions to host systems, which can have deleterious effects.[50] Therefore, it will be critical to understand how natural systems buffer cross talk such that these interactions can be engineered *de novo*.

Materials and Methods

Determination of *in vitro* rate constants

The values of the rate constants k_1–k_{10} were determined by minimizing the difference between the solution of a system of 10 linear ODEs and the 10 *in vitro* phosphotransfer curves. For each phosphotransfer reaction, we determined the analytical solution for the ODE describing the fraction of phosphorylated response regulator over time using pseudo-first-order kinetics with $C_{EnvZ,TOT} = C_{CpxA,TOT} = 1$ μM.

For OmpR phosphotransfer, with $\phi = C_{OmpR\text{-}P}/C_{OmpR,TOT}$, these equations are as follows:

1. cognate kinase: $\phi_1(t) = 1 - \exp(-k_1 C_{EnvZ;TOT} t)$
2. non-cognate kinase: $\phi_2(t) = 1 - \exp(-k_2 C_{CpxA;TOT} t)$
3. cognate phosphatase: $$\phi_3(t) = \frac{k_5 + \exp\left(-t\left(k_5 + k_3 C_{EnvZ,TOT}\right)\right) k_3 C_{EnvZ,TOT}}{k_5 + k_3 C_{EnvZ,TOT}}$$
4. non-cognate phosphatase: $$\phi_4(t) = \frac{k_5 + \exp\left(-t\left(k_5 + k_4 C_{CpxA,TOT}\right)\right) k_4 C_{CpxA,TOT}}{k_5 + k_4 C_{CpxA,TOT}}$$
5. acetyl-phosphate transfer only: $\phi_5(t) = 1 \exp(-k_5 t)$

For CpxR phosphotransfer, with $\chi = C_{CpxR\text{-}P}/C_{CpxR,TOT}$, these equations are as follows:

6. cognate kinase: $\chi_6(t) = 1 - \exp(-k_6 C_{CpxA;TOT} t)$
7. non-cognate kinase: $\chi_7(t) = 1 - \exp(-k_7 C_{EnvZ;TOT} t)$
8. cognate phosphatase: $$\chi_8(t) = \frac{k_{10} + \exp\left(-t\left(k_{10} + k_8 C_{CpxA,TOT}\right)\right) k_8 C_{CpxA,TOT}}{k_{10} + k_8 C_{CpxA,TOT}}$$
9. non-cognate phosphatase: $$\chi_9(t) = \frac{k_{10} + \exp\left(-t\left(k_{10} + k_9 C_{EnvZ,TOT}\right)\right) k_9 C_{EnvZ,TOT}}{k_{10} + k_9 C_{EnvZ,TOT}}$$
10. acetyl-phosphate transfer only: $\chi_{10}(t) = 1 - \exp(-k_{10} t)$

A Levenberg–Marquardt algorithm (Matlab, Math-Works) identifies the best-fit values of the kinetic constants by minimizing the residual, $R = \sum_{i=1}^{5}\left(\phi_i - \phi_i^{exp}\right)^2 + \sum_{i=6}^{10}\left(\chi_i - \chi_i^{exp}\right)^2$, where ϕ^{exp} and χ^{exp} are the five experimentally measured phosphotransfer curves for OmpR and CpxR, respectively. This best-fit procedure is repeated twice more using the mean ± 1 SD values of ϕ^{exp} and χ^{exp} in order to determine the range of kinetic constant values that fit within the experimental data, including the measurement error.

Solution of the *in vivo* mathematical model

The solution of the *in vivo* mathematical model is determined for each of the eight knockout scenarios (Fig. 3). The measured *in vitro* rate constants are substituted into the four ODEs described in the main text. In each knockout scenario, the rate constants corresponding to the eliminated phosphotransfer reactions are set to zero and the dynamic solution to the ODEs is determined by numerical integration (Matlab, MathWorks). To better represent the effect of an active EnvZ kinase on the dynamics, we first determined the steady-state concentration of CpxR-P in the absence of EnvZ (Fig. 3a, gray dashed lines). Starting from this steady-state concentration, an active EnvZ is added to the system at 6 min and the CpxR-P concentration profile is determined from 6 to 90 min (black lines).

Media and solutions

All cloning was performed in 2YT liquid media (31 g of 2YT per 1 L, Teknova). Selective agar plates were prepared for antibiotic selection using 25 g of Luria–Bertani broth (LB) (Miller formulation, Difco) and 18 g of Bacto Agar (Difco) per 1 L plus appropriate antibiotics (ampicillin, 100 μg/mL; kanamycin, 25 μg/mL; chloramphenicol, 25 μg/mL). Protein purification buffers used were buffer A (100 mM NaCl and 25 mM Tris–HCl, pH 7.4), buffer B (buffer A + 10 mM imidazole), and buffer C (buffer A + 300 mM imidazole). The reaction buffer contained 50 mM Tris–HCl, 50 mM KCl, and 10 mM $MgCl_2$, pH 7.4. The quench buffer contained 75 mM Tris–HCl, pH 8.0, 0.6% SDS, 1.2 mM ethylenediaminetetraacetic acid, 0.025% bromothymol blue, and 15% glycerol. *In vivo* experiments were performed in M9 media (48 mM Na_2HPO_4, 22 mM KH_2PO_4, 16 mM NH_4Cl, 2 mM $MgSO_4$, 0.1 mM $CaCl_2$, and 8.6 mM NaCl, pH 7.4) supplemented with 0.4% glucose. A total of 50 mM aspartate (Sigma) was diluted into M9 media with glucose and equilibrated to pH 7.4 before use.

Protein purification

The cytoplasmic portions of the EnvZ and CpxA kinase and the full OmpR and CpxR proteins were cloned into an in-house expression vector in front of a pBAD promoter and prior to a 6× histidine affinity tag. These constructs were transformed into OneShot DH10B cells from Invitrogen and grown for 12–16 h on ampicillin-selective LB/agar. Single colonies were used to inoculate 1 L of 2YT media (Teknova) in a 2.8-L baffled flask that was grown at 37 °C until an OD_{600} between 0.3 and 0.4, at which point the cultures were moved to 30 °C. At OD_{600} = 0.5, protein expression was induced with 10 mM arabinose and cultures were grown for 12–16 h. Cells were pelleted by spinning at 3738*g* for 20 min and resuspended in 25 mL of buffer A. After addition of lysozyme, cells were frozen at –20 deg overnight, thawed, and sonicated using a Sonic Dismembrator Model 500 (Fisher Scientific) four times for 30 s each, with 1-s intervals at 25% amplitude. Lysate was cleared by spinning at 19,647*g* for 30 min, after which it was exposed to a 0.8 μM filter (NALGENE) and incubated with 1 mL of TALON resin (Clonetech) at 4 deg with gentle shaking for 1–2 h. Lysate plus resin was poured into a 50-mL column (BioRad) and was allowed to settle. Column was washed with 25 mL of buffer A and 25 mL of buffer B and eluted with 10 mL of buffer C, diluted twofold with buffer A. Elution was dialyzed into a storage buffer, and protein was concentrated using an Amicon Ultra-4 Ultracel 10K centrifugal filter device (Millipore). Final protein concentration was obtained by taking the absorbance reading at A_{280} using an extinction coefficient calculated using the method of Gill and von Hippel.[79] Glycerol was added to a final concentration of 18.75%, and samples were stored at –80 until use.

Kinase phosphorylation

Kinase was diluted to a final concentration of 2 μM in 200 μL of reaction buffer supplemented with 100 μCi of [γ-^{32}P]ATP (~6000 Ci/mmol; MP Biomedicals), and the reaction was incubated at 37 °C for 40 min, 10 min past the saturation point of the kinase

autophosphorylation (data not shown). The protein solution was then diluted to 600 μL using cold reaction buffer and moved to a Microcon Ultracel YM-10 (Millipore). The solution was spun through the filter at 14,000g for 20 min, after which 400 μL of cold reaction buffer was added. This was repeated three times, with the final spin 22 min long. Kinase was diluted to 2 μM with cold reaction buffer.

Non-cognate response regulator phosphorylation

Phosphorylated kinase was diluted to 1 μM into a solution containing 10 μM concentration of the non-cognate response regulator protein, and 9 μL was removed immediately as the zero point in the reaction. Nine-microliter aliquots were removed at specified time points, mixed with 9 μL of 2× SDS loading buffer, and kept on ice until all reactions were complete. Fifteen-microliter samples were then loaded into 12-well 12% Tris–glycine SDS-PAGE gels (Lonza) without boiling and run for 1 h 10 min at 20 mA per gel (Bio-Rad). Gels were dried using a Model 583 Gel Dryer (Bio-Rad) and exposed to a Kodak Storage Phosphor Screen (Amersham Biosciences) for 12–16 h before they were imaged using a Typhoon 9400 imaging system (Amersham Biosciences). Densitometry analysis was performed using the free software ImageJ.[80] All numbers within a certain experiment were normalized to the highest value for radiolabeled protein using Microsoft Excel. This provided a number for the fraction of protein phosphorylated, which was used as input for the kinetic calculations. Values are the mean of four independent experiments, and error bars represent one standard deviation from the mean.

Cognate response regulator phosphorylation

Phosphorylated kinase was diluted to a final concentration of 2 μM in reaction buffer. Response regulator was diluted to 20 μM in reaction buffer. Kinase and response regulator (~ 17.5 μL each) were mixed and quickly exposed to 82.5 μL of quench buffer after a specified amount of time using a Rapid Quench Flow System (KinTek Corporation). Samples were kept on ice until 15 μL was removed for electrophoreses. Data analysis was as described above.

Synthesis of ^{32}P-labeled acetyl phosphate

The synthesis method was adapted from the method of McCleary and Stock.[63] In total, 0.240 mL of pyridine, 0.063 mL of 2 M K_2HPO_4, and 0.500 mL of carrier-free orthophosphate (MP Biomedicals) were combined in a 15-mL FALCON tube and placed on ice for at least 10 min. Over the next 2 min, 0.0275 mL of acetic anhydride was added while the reaction was being mixed on ice. A total of 0.108 mL of 4 N LiOH was then added, and the reaction was mixed for 3 min more on ice before addition of 5.75 mL of cold 100% ethanol. The reaction was left to incubate on ice for 1 h to precipitate product. Product was isolated by spinning at 2851*g* for 10 min and discarding the supernatant, followed by two more washes with 6.0 mL of 100% ethanol. White precipitate was resuspended in 0.75 mL of water, and 0.35 mL of cold ethanol was added. After a 15-min incubation on ice, reaction was spun at 2851*g* for 10 min and supernatant was collected while precipitate containing impurities was discarded. A total of 5.0 mL of cold ethanol was added to precipitate acetyl phosphate, and precipitate was collected by spinning at 2851*g* for 10 min. Purified acetyl phosphate was resuspended in 0.200 mL of 100 mM Tris–HCl, pH 7.0. Acetyl phosphate was stored at –20 °C and used within 1 week of synthesis. The synthesis method was refined and optimized using K_2HPO_4 and comparing with a standard solution of acetyl phosphate (Sigma Aldrich). NMR spectra of synthesized product and purchased product were identical. NMR spectra of the radioactive product were not taken for safety reasons.

Kinase-independent response regulator phosphorylation

Response regulator protein was diluted to a concentration of 20 μM in 90 μL of reaction buffer and 10 μL of acetyl phosphate and incubated at 37 °C. Nine-microliter aliquots were removed

at specified time points and mixed with 9 μL of SDS loading buffer, 15 μL of which was electrophoresed and imaged in the same fashion as previously described.

Response regulator dephosphorylation

A total of 20 μM response regulator protein was incubated in 90 μL of reaction buffer plus 10 μL of ^{32}P-labeled acetyl phosphate for 40 min at 37 °C. Afterward, kinase was added to a final concentration of 2 μM with 1 mM ADP and 9-μL aliquots were removed at specified time points, mixed with 9 μL of SDS loading buffer, and placed on ice. A total of 15 μL was removed and electrophoresed in the same method as described previously.

Genomic knockouts

Strain BW28357 was obtained from the Coli Genetic Stock Center at Yale, and all genes were knocked out according to the method of Datsenko and Wanner.[81] After confirming each knockout with genomic sequencing, we used P1 phage to transfer each knockout to a recombinase-free strain of BW28357. After knocking out the gene of interest, we removed the kanamycin antibiotic resistance marker using plasmid pcp20 according to the method of Datsenko and Wanner. All strains were confirmed to be sensitive to kanamycin.

Plasmid construction

The *ompC* promoter region was amplified from the *E. coli* genomic DNA using the primers gcggccgcATGAAAAGTGTGTAAAGAAGGGT and ggatccGTTATTAACCCTCTGTTATATGCCTTTATTTGC. It was subsequently cut with NotI and BamHI (New England Biolabs) before ligating into plasmid pAC581 immediately prior to GFP Mut3 v.JCA (courtesy of Professor John C. Anderson at the University of California, Berkeley). The *cpxP* promoter was prepared in a similar fashion using the primers GCGGCCGCTAATAGGGAAGTCAGCTCTCGGTCATC and GGATCCTTCAGCAGCGTGGCTTAATGAACTGACTGC. Both constructs were shown to be highly selective reporters for the OmpR-P and CpxR-P proteins, respectively (data not shown). The TAZ construct was contained on plasmid pTJ003 (courtesy of Masayori Inouye).

Fluorescent measurements and cytometry

Cells were transformed with pAC581-PompC-GFP, pAC581-PcpxP-GFP, or plasmid and pTJ003 and grown for 12–16 h at 37 °C on selective LB/agar. Control cells containing no plasmid, used to normalize cell fluorescence, were grown for 12–16 h at 37 °C on LB/agar as well. Single colonies were used to inoculate overnight (12–16 h) cultures of 2 mL of M9 media supplemented with appropriate antibiotics. Next, the cultures were diluted 100× into 50 mL of fresh M9 with appropriate antibiotics and grown at 37 °C in a shaking water bath to OD_{600} = 0.2. They were then split, and 18 mL was put into each of two flasks and exposed to 2 mL of either pre-warmed M9 media or pre-warmed M9 media supplemented with 50 mM aspartate, for a final aspartate concentration of 5 mM. Cells were grown at 37 °C with shaking for 2 h more post-induction. Samples were taken, spun at 3300*g* for 5 min, and resuspended in 1× phosphate-buffered saline with kanamycin (2 mg/mL) to stop translation. Cells were diluted into 1× phosphate-buffered saline, and single-cell GFP measurements were made using a BD Biosciences LSRII, courtesy of the Gladstone Research Institute (laser settings: FSC, 577; SSC, 335; GFP, 607). Each data set consisted of at least 30,000 bacteria. The FlowJo software package was used to gate the data by FSC-H and SSC-A before calculating a geometric mean GFP fluorescence value (Tree Star Inc.).

Supplementary Material

Refer to Web version on PubMed Central for supplementary material.

Acknowledgments

C.A.V. was supported by the Office of Naval Research, the Pew Fellowship Program, the Packard Fellowship Program, the National Institutes of Health (EY016546 and AI067699), the National Science Foundation (BES-0547637), UC-Discovery, a Sandler Family Opportunity Award, and the SynBERC National Science Foundation Engineering Research Center (www.synberc.org). E.S.G. was supported by a Burroughs Wellcome Fellowship.

Abbreviations used

ODE	ordinary differential equation
WT	wild type
GFP	green fluorescent protein

References

1. Kofoid EC, Parkinson JS. Transmitter and receiver modules in bacterial signaling proteins. Proc. Natl Acad. Sci. USA 1988;85:4981–4985. [PubMed: 3293046]
2. Parkinson JS, Kofoid EC. Communication modules in bacterial signaling proteins. Annu. Rev. Genet 1992;26:71–112. [PubMed: 1482126]
3. Hoch, JA.; Silhavy, TJ. Two-Component Signal Transduction. ASM Press; Herndon, VA: 1995.
4. Aiba H, Mizuno T, Mizushima S. Transfer of phosphoryl group between two regulatory proteins involved in osmoregulatory expression of the *ompF* and *ompC* genes in *Escherichia coli*. J. Biol. Chem 1989;264:8563–8567. [PubMed: 2656684]
5. Ronson CW, Nixon BT, Ausubel FM. Conserved domains in bacterial regulatory proteins that respond to environmental stimuli. Cell 1987;49:579–581. [PubMed: 3555840]
6. Ninfa AJ, Magasanik B. Covalent modification of the *glnG* product, NR_I, by the *glnL* product, NR_{II}, regulates the transcription of the *glnALG* operon in *Escherichia coli*. Proc. Natl Acad. Sci. USA 1986;83:5909–5913. [PubMed: 2874557]
7. Aiba H, Mizuno T. Phosphorylation of a bacterial activator protein, OmpR, by a protein kinase, EnvZ, stimulates the transcription of the *ompF* and *ompC* genes in *Escherichia coli*. FEBS Lett 1990;261:19–22. [PubMed: 2407554]
8. Forst S, Delgado J, Inouye M. Phosphorylation of OmpR by the osmosensor EnvZ modulates expression of the *ompF* and *ompC* genes in *Escherichia coli*. Proc. Natl Acad. Sci. USA 1989;86:6052–6056. [PubMed: 2668953]
9. Hazelbauer GL, Berg HC, Matsumura P. Bacterial motility and signal transduction. Cell 1993;73:15–22. [PubMed: 8096433]
10. Francez-Charlot A, Laugel B, Van Gemert A, Dubarry N, Wiorowski F, Castanie-Cornet MP, et al. RcsCDB His–Asp phosphorelay system negatively regulates the *flhDC* operon in *Escherichia coli*. Mol. Microbiol 2003;49:823–832. [PubMed: 12864862]
11. Shin S, Park C. Modulation of flagellar expression in *Escherichia coli* by acetyl phosphate and the osmoregulator OmpR. J. Bacteriol 1995;177:4696–4702. [PubMed: 7642497]
12. Kleerebezem M, Quadri LE, Kuipers OP, de Vos WM. Quorum sensing by peptide pheromones and two-component signal-transduction systems in Gram-positive bacteria. Mol. Microbiol 1997;24:895–904. [PubMed: 9219998]
13. Li YH, Lau PC, Tang N, Svensater G, Ellen RP, Cvitkovitch DG. Novel two-component regulatory system involved in biofilm formation and acid resistance in *Streptococcus mutans*. J. Bacteriol 2002;184:6333–6342. [PubMed: 12399503]
14. Garmendia J, Beuzon CR, Ruiz-Albert J, Holden DW. The roles of SsrA–SsrB and OmpR–EnvZ in the regulation of genes encoding the *Salmonella typhimurium* SPI-2 type III secretion system. Microbiology 2003;149:2385–2396. [PubMed: 12949164]
15. Dorel C, Vidal O, Prigent-Combaret C, Vallet I, Lejeune P. Involvement of the Cpx signal transduction pathway of *E. coli* in biofilm formation. FEMS Microbiol. Lett 1999;178:169–175. [PubMed: 10483736]

16. Rabin RS, Stewart V. Dual response regulators (NarL and NarP) interact with dual sensors (NarX and NarQ) to control nitrate- and nitrite-regulated gene expression in *Escherichia coli* K-12. J. Bacteriol 1993;175:3259–3268. [PubMed: 8501030]

17. Jung K, Hamann K, Revermann A. K^+ stimulates specifically the autokinase activity of purified and reconstituted EnvZ of *Escherichia coli*. J. Biol. Chem 2001;276:40896–40902. [PubMed: 11533042]

18. Ferrieres L, Clarke DJ. The RcsC sensor kinase is required for normal biofilm formation in *Escherichia coli* K-12 and controls the expression of a regulon in response to growth on a solid surface. Mol. Microbiol 2003;50:1665–1682. [PubMed: 14651646]

19. Ullrich M, Penaloza-Vazquez A, Bailey AM, Bender CL. A modified two-component regulatory system is involved in temperature-dependent biosynthesis of the *Pseudomonas syringae* phytotoxin coronatine. J. Bacteriol 1995;177:6160–6169. [PubMed: 7592381]

20. Yeh KC, Wu SH, Murphy JT, Lagarias JC. A cyanobacterial phytochrome two-component light sensory system. Science 1997;277:1505–1508. [PubMed: 9278513]

21. Hirakawa H, Inazumi Y, Masaki T, Hirata T, Yamaguchi A. Indole induces the expression of multidrug exporter genes in *Escherichia coli*. Mol. Microbiol 2005;55:1113–1126. [PubMed: 15686558]

22. Sato M, Machida K, Arikado E, Saito H, Kakegawa T, Kobayashi H. Expression of outer membrane proteins in *Escherichia coli* growing at acid pH. Appl. Environ. Microbiol 2000;66:943–947. [PubMed: 10698756]

23. Yamamoto K, Ishihama A. Transcriptional response of *Escherichia coli* to external copper. Mol. Microbiol 2005;56:215–227. [PubMed: 15773991]

24. Mascher T, Zimmer SL, Smith TA, Helmann JD. Antibiotic-inducible promoter regulated by the cell envelope stress-sensing two-component system LiaRS of *Bacillus subtilis*. Antimicrob. Agents Chemother 2004;48:2888–2896. [PubMed: 15273097]

25. David M, Daveran ML, Batut J, Dedieu A, Domergue O, Ghai J, et al. Cascade regulation of *nif* gene expression in *Rhizobium meliloti*. Cell 1988;54:671–683. [PubMed: 2842062]

26. Carballes F, Bertrand C, Bouche JP, Cam K. Regulation of *Escherichia coli* cell division genes *ftsA* and *ftsZ* by the two-component system *rcsC–rcsB*. Mol. Microbiol 1999;34:442–450. [PubMed: 10564486]

27. Rosenfeld N, Young JW, Alon U, Swain PS, Elowitz MB. Accurate prediction of gene feedback circuit behavior from component properties. Mol. Syst. Biol 2007;3:143. [PubMed: 18004276]

28. Bashor CJ, Helman NC, Yan S, Lim WA. Using engineered scaffold interactions to reshape MAP kinase pathway signaling dynamics. Science 2008;319:1539–1543. [PubMed: 18339942]

29. Dueber JE, Mirsky EA, Lim WA. Engineering synthetic signaling proteins with ultra-sensitive input/output control. Nat. Biotechnol 2007;25:660–662. [PubMed: 17515908]

30. Dueber JE, Yeh BJ, Chak K, Lim WA. Reprogramming control of an allosteric signaling switch through modular recombination. Science 2003;301:1904–1908. [PubMed: 14512628]

31. Buckler DR, Zhou Y, Stock AM. Evidence of intradomain and interdomain flexibility in an OmpR/PhoB homolog from *Thermotoga maritima*. Structure 2002;10:153–164. [PubMed: 11839301]

32. Gouet P, Fabry B, Guillet V, Birck C, Mourey L, Kahn D, Samama JP. Structural transitions in the FixJ receiver domain. Structure 1999;7:1517–1526. [PubMed: 10647182]

33. Sola M, Gomis-Ruth FX, Serrano L, Gonzalez A, Coll M. Three-dimensional crystal structure of the transcription factor PhoB receiver domain. J. Mol. Biol 1999;285:675–687. [PubMed: 9878437]

34. Volz K, Matsumura P. Crystal structure of *Escherichia coli* CheY refined at 1.7-Å resolution. J. Biol. Chem 1991;266:15511–15519. [PubMed: 1869568]

35. Utsumi R, Brissette RE, Rampersaud A, Forst SA, Oosawa K, Inouye M. Activation of bacterial porin gene expression by a chimeric signal transducer in response to aspartate. Science 1989;245:1246–1249. [PubMed: 2476847]

36. Baumgartner JW, Kim C, Brissette RE, Inouye M, Park C, Hazelbauer GL. Transmembrane signalling by a hybrid protein: communication from the domain of chemoreceptor Trg that recognizes sugar-binding proteins to the kinase/phosphatase domain of osmosensor EnvZ. J. Bacteriol 1994;176:1157–1163. [PubMed: 8106326]

37. Looger LL, Dwyer MA, Smith JJ, Hellinga HW. Computational design of receptor and sensor proteins with novel functions. Nature 2003;423:185–190. [PubMed: 12736688]

38. Levskaya A, Chevalier AA, Tabor JJ, Simpson ZB, Lavery LA, Levy M, et al. Synthetic biology: engineering *Escherichia coli* to see light. Nature 2005;438:441–442. [PubMed: 16306980]
39. Ward SM, Delgado A, Gunsalus RP, Manson MD. A NarX–Tar chimera mediates repellent chemotaxis to nitrate and nitrite. Mol. Microbiol 2002;44:709–719. [PubMed: 11994152]
40. Dwyer MA, Looger LL, Hellinga HW. Computational design of a Zn^{2+} receptor that controls bacterial gene expression. Proc. Natl Acad. Sci. USA 2003;100:11255–11260. [PubMed: 14500902]
41. Laub MT, Goulian M. Specificity in two-component signal transduction pathways. Annu. Rev. Genet 2007;41:121–145. [PubMed: 18076326]
42. Skerker JM, Perchuk BS, Siryaporn A, Lubin EA, Ashenberg O, Goulian M, Laub MT. Rewiring the specificity of two-component signal transduction systems. Cell 2008;133:1043–1054. [PubMed: 18555780]
43. Stock JB, Ninfa AJ, Stock AM. Protein phosphorylation and regulation of adaptive responses in bacteria. Microbiol. Rev 1989;53:450–490. [PubMed: 2556636]
44. Hellingwerf KJ. Bacterial observations: a rudimentary form of intelligence? Trends Microbiol 2005;13:152–158. [PubMed: 15817384]
45. Hellingwerf KJ, Postma PW, Tommassen J, Westerhoff HV. Signal transduction in bacteria: phospho-neural network(s) in *Escherichia coli*? FEMS Microbiol. Rev 1995;16:309–321. [PubMed: 7654406]
46. Alves R, Savageau MA. Comparative analysis of prototype two-component systems with either bifunctional or monofunctional sensors: differences in molecular structure and physiological function. Mol. Microbiol 2003;48:25–51. [PubMed: 12657043]
47. Siryaporn A, Goulian M. Cross-talk suppression between the CpxA–CpxR and EnvZ–OmpR two-component systems in *E. coli*. Mol. Microbiol 2008;70:494–506. [PubMed: 18761686]
48. Grimshaw CE, Huang S, Hanstein CG, Strauch MA, Burbulys D, Wang L, et al. Synergistic kinetic interactions between components of the phosphorelay controlling sporulation in *Bacillus subtilis*. Biochemistry 1998;37:1365–1375. [PubMed: 9477965]
49. Yamamoto K, Hirao K, Oshima T, Aiba H, Utsumi R, Ishihama A. Functional characterization *in vitro* of all two-component signal transduction systems from *Escherichia coli*. J. Biol. Chem 2005;280:1448–1456. [PubMed: 15522865]
50. Skerker JM, Prasol MS, Perchuk BS, Biondi EG, Laub MT. Two-component signal transduction pathways regulating growth and cell cycle progression in a bacterium: a system-level analysis. PLoS Biol 2005;3:e334. [PubMed: 16176121]
51. Dong J, Iuchi S, Kwan HS, Lu Z, Lin EC. The deduced amino-acid sequence of the cloned *cpxR* gene suggests the protein is the cognate regulator for the membrane sensor, CpxA, in a two-component signal transduction system of *Escherichia coli*. Gene 1993;136:227–230. [PubMed: 8294007]
52. De Wulf P, McGuire AM, Liu X, Lin EC. Genome-wide profiling of promoter recognition by the two-component response regulator CpxR-P in *Escherichia coli*. J. Biol. Chem 2002;277:26652–26661. [PubMed: 11953442]
53. Raivio TL. Envelope stress responses and Gram-negative bacterial pathogenesis. Mol. Microbiol 2005;56:1119–1128. [PubMed: 15882407]
54. Batchelor E, Walthers D, Kenney LJ, Goulian M. The *Escherichia coli* CpxA–CpxR envelope stress response system regulates expression of the porins *ompF* and *ompC*. J. Bacteriol 2005;187:5723–5731. [PubMed: 16077119]
55. Altschul SF, Gish W, Miller W, Myers EW, Lipman DJ. Basic local alignment search tool. J. Mol. Biol 1990;215:403–410. [PubMed: 2231712]
56. Igo MM, Ninfa AJ, Stock JB, Silhavy TJ. Phosphorylation and dephosphorylation of a bacterial transcriptional activator by a transmembrane receptor. Genes Dev 1989;3:1725–1734. [PubMed: 2558046]
57. Jin T, Inouye M. Ligand binding to the receptor domain regulates the ratio of kinase to phosphatase activities of the signaling domain of the hybrid *Escherichia coli* transmembrane receptor, Taz1. J. Mol. Biol 1993;232:484–492. [PubMed: 8393937]
58. Ninfa AJ, Ninfa EG, Lupas AN, Stock A, Magasanik B, Stock J. Crosstalk between bacterial chemotaxis signal transduction proteins and regulators of transcription of the Ntr regulon: evidence that nitrogen assimilation and chemotaxis are controlled by a common phosphotransfer mechanism. Proc. Natl Acad. Sci. USA 1988;85:5492–5496. [PubMed: 3041412]

59. De Wulf P, Lin EC. Cpx two-component signal transduction in *Escherichia coli*: excessive CpxR-P levels underlie CpxA* phenotypes. J. Bacteriol 2000;182:1423–1426. [PubMed: 10671468]
60. Wolfe AJ, Parikh N, Lima BP, Zemaitaitis B. Signal integration by the two-component signal transduction response regulator CpxR. J. Bacteriol 2008;190:2314–2322. [PubMed: 18223085]
61. Igo MM, Silhavy TJ. EnvZ, a transmembrane environmental sensor of *Escherichia coli* K-12, is phosphorylated in vitro. J. Bacteriol 1988;170:5971–5973. [PubMed: 3056929]
62. Ames SK, Frankema N, Kenney LJ. C-terminal DNA binding stimulates N-terminal phosphorylation of the outer membrane protein regulator OmpR from *Escherichia coli*. Proc. Natl Acad. Sci. USA 1999;96:11792–11797. [PubMed: 10518529]
63. McCleary WR, Stock JB. Acetyl phosphate and the activation of two-component response regulators. J. Biol. Chem 1994;269:31567–31572. [PubMed: 7989325]
64. Yoshida T, Cai S, Inouye M. Interaction of EnvZ, a sensory histidine kinase, with phosphorylated OmpR, the cognate response regulator. Mol. Microbiol 2002;46:1283–1294. [PubMed: 12453215]
65. Cai SJ, Inouye M. EnvZ–OmpR interaction and osmoregulation in *Escherichia coli*. J. Biol. Chem 2002;277:24155–24161. [PubMed: 11973328]
66. Wolfe AJ. The acetate switch. Microbiol. Mol. Biol. Rev 2005;69:12–50. [PubMed: 15755952]
67. Maeda S, Mizuno T. Evidence for multiple OmpR-binding sites in the upstream activation sequence of the *ompC* promoter in *Escherichia coli*: a single OmpR-binding site is capable of activating the promoter. J. Bacteriol 1990;172:501–503. [PubMed: 2403550]
68. Yamamoto K, Ishihama A. Characterization of copper-inducible promoters regulated by CpxA/CpxR in *Escherichia coli*. Biosci., Biotechnol., Biochem 2006;70:1688–1695. [PubMed: 16861804]
69. Batchelor E, Silhavy TJ, Goulian M. Continuous control in bacterial regulatory circuits. J. Bacteriol 2004;186:7618–7625. [PubMed: 15516575]
70. Otto K, Silhavy TJ. Surface sensing and adhesion of *Escherichia coli* controlled by the Cpx-signaling pathway. Proc. Natl Acad. Sci. USA 2002;99:2287–2292. [PubMed: 11830644]
71. Batchelor E, Goulian M. Imaging OmpR localization in *Escherichia coli*. Mol. Microbiol 2006;59:1767–1778. [PubMed: 16553882]
72. Fabret C, Feher A, Hoch JA. Two-component signal transduction in *Bacillus subtilis*: how one organism sees its world. J. Bacteriol 1999;181:1975–1983. [PubMed: 10094672]
73. Jiang M, Shao W, Perego M, Hoch JA. Multiple histidine kinases regulate entry into stationary phase and sporulation in *Bacillus subtilis*. Mol. Microbiol 2000;38:535–542. [PubMed: 11069677]
74. Zhou L, Lei XH, Bochner BR, Wanner BL. Phenotype microarray analysis of *Escherichia coli* K-12 mutants with deletions of all two-component systems. J. Bacteriol 2003;185:4956–4972. [PubMed: 12897016]
75. Jubelin G, Vianney A, Beloin C, Ghigo JM, Lazzaroni JC, Lejeune P, Dorel C. CpxR/OmpR interplay regulates curli gene expression in response to osmolarity in *Escherichia coli*. J. Bacteriol 2005;187:2038–2049. [PubMed: 15743952]
76. Oshima T, Aiba H, Masuda Y, Kanaya S, Sugiura M, Wanner BL, et al. Transcriptome analysis of all two-component regulatory system mutants of *Escherichia coli* K-12. Mol. Microbiol 2002;46:281–291. [PubMed: 12366850]
77. Mattison K, Kenney LJ. Phosphorylation alters the interaction of the response regulator OmpR with its sensor kinase EnvZ. J. Biol. Chem 2002;277:11143–11148. [PubMed: 11799122]
78. Voigt CA. Genetic parts to program bacteria. Curr. Opin. Biotechnol 2006;17:548–557. [PubMed: 16978856]
79. Gill SC, von Hippel PH. Calculation of protein extinction coefficients from amino acid sequence data. Anal. Biochem 1989;182:319–326. [PubMed: 2610349]
80. Abramoff MD, Magelhaes PJ, Ram SJ. Image processing with ImageJ. Biophoton. Int 2004;11:36–42.
81. Datsenko KA, Wanner BL. One-step inactivation of chromosomal genes in *Escherichia coli* K-12 using PCR products. Proc. Natl Acad. Sci. USA 2000;97:6640–6645. [PubMed: 10829079]

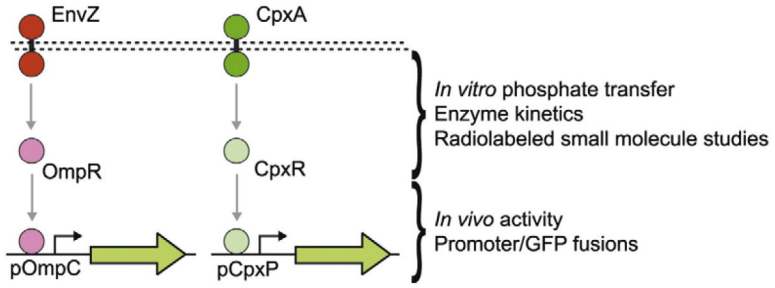

Fig. 1.

Overview of the EnvZ/OmpR and CpxA/CpxR two-component systems. The EnvZ and CpxA histidine kinases (red and green, respectively) reside in the inner membrane and respond to a variety of signals. Upon activation, these kinases autophosphorylate and transfer a phosphate to their cognate response regulators, OmpR and CpxR (pink and light green circles, respectively). Upon phosphorylation, OmpR-P and CpxR-P activate the *ompC* and *cpxP* promoters, respectively. We measured the phosphorelay kinetics *in vitro* using radiolabeled phosphate and purified proteins. The downstream effects were measured *in vivo* using promoter-GFP transcriptional fusions and flow cytometry.

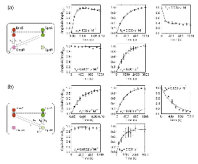

Fig. 2.

In vitro kinetic analysis of the EnvZ/OmpR and CpxA/CpxR systems. All of the phosphotransfer reactions affecting OmpR (a) and CpxR (b) are shown. The data for each reaction were extracted from gel assays and are shown as the fraction of response regulator phosphorylated at each time point. Points are the average of four experiments, and error bars are a single standard deviation from the mean. The continuous lines were obtained by fitting the fraction of phosphorylated response regulator to a mathematical model of the phosphotransfer assays, yielding the values of the best-fit rate constants for each reaction. All rate constants, as well as error for each of these values, are shown in Table 1.

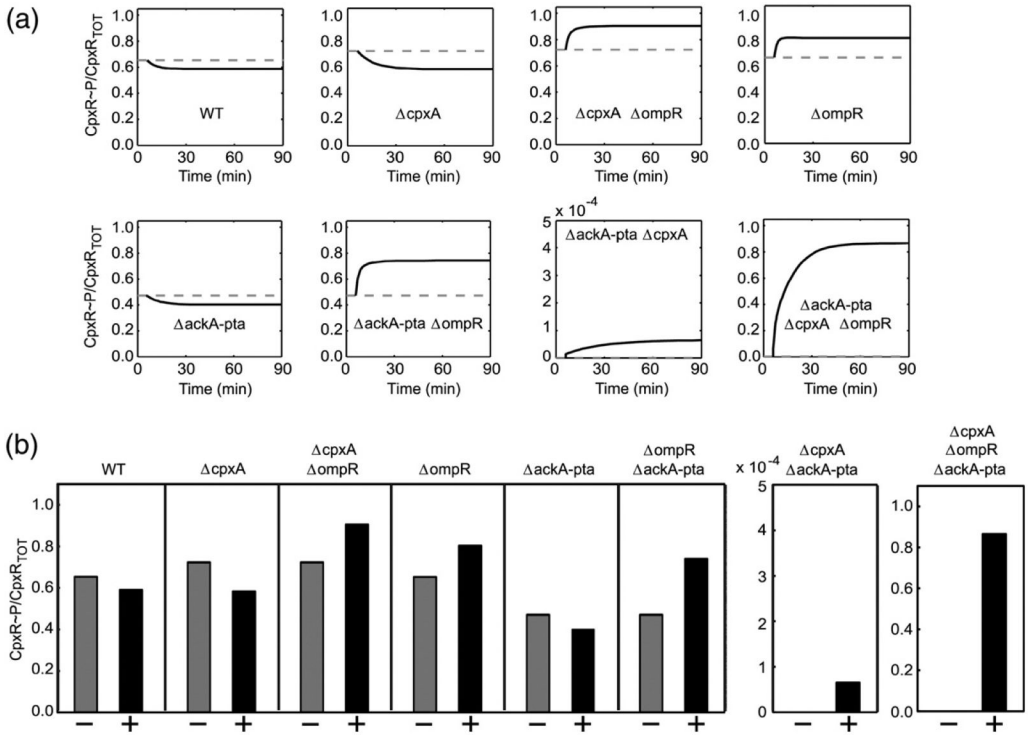

Fig. 3.

Kinetic model of CpxR phosphorylation *in vivo*. The effect of knocking out various components of the pathways is shown. The solution of the model describes the fraction of phosphorylated CpxR after EnvZ is activated. (a) Time series demonstrate the dynamics of CpxR-P from 0 to 90 min post-induction under each knockout scenario. The model solutions in the absence of active EnvZ are allowed to reach steady state (gray dashed line) and then EnvZ is activated at the 6-min time point (black line). (b) The bar graphs show the final steady-state fraction of CpxR-P in the absence (gray) or in the presence (black) of active EnvZ.

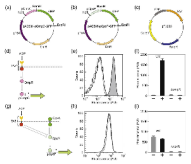

Fig. 4.

In vivo measurement system for response regulator phosphorylation. Plasmid maps are shown for the reporter systems: (a) pAC581-pOmpC-GFP and (b) pAC581-pCpxP-GFP, which contain the *ompC* and *cpxP* promoters driving GFP expression. (c) The reporters are co-transformed with a second plasmid, pTJ003, which contains the TAZ protein under control of the constitutive *lpp* promoter. (d) TAZ phosphorylates OmpR in the presence of 5 mM asparate. (e) Gated cytometry data are shown for cells without TAZ (gray line) and with TAZ but without asparate (black line). Addition of 5 mM aspartate induces the system (black line with gray fill, right). (f) The *ompC* reporter is not induced in the absence of TAZ (–) but is strongly induced when both TAZ and aspartate are present (+). When ompR is knocked out, TAZ has no affect on the system. (g) The ability of TAZ to induce CpxR was also measured in wild-type cells. (h) The cytometry distribution shows no difference between cells with TAZ and aspartate (black line) and cells without TAZ (gray line). There is a basal level of activity from the *cpxP* promoter. (i) The activity of the *cpxP* promoter is the same in the absence (–) and in the presence (+) of TAZ and inducer. The basal activity is eliminated by knocking out CpxR. For both (f) and (i), the mean of three experiments performed on different days is shown and the error bars are one standard deviation from the mean.

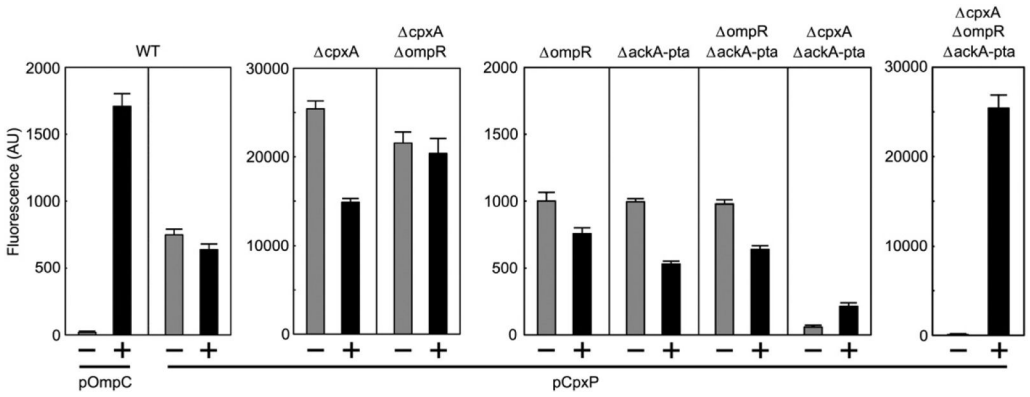

Fig. 5.

in vivo experiments measuring cross talk when various component genes are knocked out. The first two panels show data for the strains where only EnvZ is knocked out, which is labeled "WT." The additional knockouts are shown at the top of each panel, and the promoter used as a reporter is shown at the bottom. For each knockout, the fluorescence in the absence of EnvZ (–) and that in the presence of active EnvZ kinase (TAZ and aspartate) (+) are shown. Only a triple knockout, Δ*ackA-pta* Δ*cpxA* Δ*ompR*, displays strong cross talk. Error bars represent the mean of three experiments, and the error bars are one standard deviation from the mean.

Table 1

In vitro kinetic parameters

Kinetic constant	Best fit	Range[a]	Reaction
k_1	102.1 $s^{-1}M^{-1}$	±7.7	Cognate kinase activity by EnvZ
k_2	0.0031 $s^{-1}M^{-1}$	$\pm 4 \times 10^{-4}$	Non-cognate kinase activity by CpxA
k_3	0.00294 $s^{-1}M^{-1}$	$\pm 6 \times 10^{-5}$	Cognate phosphatase activity by EnvZ
k_4	0.00010 $s^{-1}M^{-1}$	$\pm 2 \times 10^{-5}$	Non-cognate phosphatase activity by CpxA
k_5	0.0011 s^{-1}	$\pm 3 \times 10^{-4}$	Acetyl-phosphate transfer onto OmpR
k_6	28.5 $s^{-1}M^{-1}$	±6.8	Cognate kinase activity by CpxA
k_7	0.0031 $s^{-1}M^{-1}$	$\pm 4 \times 10^{-4}$	Non-cognate kinase activity by EnvZ
k_8	0.0030 $s^{-1}M^{-1}$	$\pm 3 \times 10^{-4}$	Cognate phosphatase activity by CpxA
k_9	0.0015 $s^{-1}M^{-1}$	$\pm 1.45 \times 10^{-3}$	Non-cognate phosphatase activity by EnvZ
k_{10}	0.0011 s^{-1}	$\pm 3 \times 10^{-4}$	Acetyl-phosphate transfer onto CpxR

[a] Range of kinetic constant values due to measurement error (see Materials and Methods).